Biophysical Journal Volume 90 February 2006 1329–1337

Unique Properties of Purine/Pyrimidine Asymmetric PNA·DNA Duplexes: Differential Stabilization of PNA·DNA Duplexes by Purines in the PNA Strand

Anjana Sen and Peter E. Nielsen

Department of Medical Biochemistry and Genetics, Faculty of Health Sciences, University of Copenhagen, The Panum Institute, Copenhagen, Denmark

ABSTRACT PNA·DNA duplexes are significantly stabilized by purine nucleobases in the PNA strand. To elucidate and understand the effect of switching the backbone in a nucleic acid duplex, we now report a thermodynamics study along with a solution conformations study of two purine/pyrimidine strand asymmetric duplexes and a strand symmetrical control by comparing the behavior of all four possible PNA/DNA combinations. In essence, we are comparing an identical basepair stack connected by either an aminoethyl glycine PNA or a deoxyribose DNA backbone. We show that the PNA·DNA duplexes containing purine-rich PNA strands are stabilized with regard to the thermal melting temperature and free energy as well as enthalpy (and concomitantly relatively less entropically disfavored). Based on our data, we find it unlikely that differences in counterion binding (identical ionic-strength dependence was observed), hydration (identical and insignificant water release was observed), or single-strand conformation can be responsible for the difference in duplex stability. The only consistent difference observed between the purine-rich PNA versus the pyrimidine-rich PNA in isosequential PNA·DNA duplexes is the significant increase in both binding enthalpy and entropy for the PNA·DNA duplexes containing pyrimidine-rich PNA in organic solvent, which would indicate that these duplexes are relatively enthalpically disfavored in water. Although our results so far do not allow us to identify the origin of the different stabilities of homopurine/homopyrimidine PNA·DNA duplexes, the evidence does point to a significant structural component, which involves enthalpic contributions both within the duplex structure and also from bound water molecules.

INTRODUCTION

Heteroduplexes between peptide nucleic acids (PNA) and DNA are in general both thermally and thermodynamically more stable than isosequential DNA·DNA duplexes (1–13). However, the sequence dependence of PNA·DNA duplex stability is more complex than that of pure DNA duplexes. In addition to stabilization by G·C basepair content, the duplexes are considerably stabilized when the purines are present in the PNA strand rather than in the DNA strand (13,14). For example, it was found that for a pure homopurine/homopyrimidine sequence, the thermal stability of a decamer PNA(pur)·DNA(pyr) duplex is ~70°C (14), whereas that of a decamer PNA(pyr)·DNA(pur) duplex is typically at ~30°C (15). Therefore, duplex stability is critically influenced by the backbone chemistry in an asymmetric way.

Analogous observations have previously been described for DNA·RNA duplexes but the effects are of much smaller magnitude (16,17). Furthermore, these complexes also differ in nucleobase composition and consequently in stacking interactions, as thymine is substituted for uracil in the RNA strands. Comparison of the thermodynamic stabilities and solution conformations of DNA·RNA hybrids containing purine-rich and pyrimidine-rich strands with DNA and RNA duplexes along with their DNA and RNA homoduplex partners have been elaborately investigated by Brown and co-workers (16,17). Based on NMR analysis, these authors ascribed the stability differences predominantly to structural and dynamic differences between the duplexes, though a detailed molecular understanding is not apparent.

To further elucidate and understand the effect of switching the backbone in a nucleic acid duplex, we now report a thermodynamics study along with a solution conformations study of two purine/pyrimidine strand asymmetric duplexes and a strand symmetrical control by comparing the behavior of all four possible PNA/DNA combinations. Thus, in essence we are comparing an identical basepair stack connected by either an aminoethyl glycine PNA or a deoxyribose DNA backbone.

MATERIALS AND METHODS

PNAs

PNA1, PNA2, PNA3, PNA4, PNA5, and PNA6 were synthesized and characterized using solid-phase Boc chemistry and purified by HPLC, as described previously (18). PNA concentrations were determined spectrophotometrically at 65°C using molar extinction coefficients for the corresponding deoxyribonucleotides: ε_{260} of adenine = 15,400 M^{-1} cm^{-1}, ε_{260} of guanine = 11,700 M^{-1} cm^{-1}, ε_{260} of thymine = 8800 M^{-1} cm^{-1}, and ε_{260} of cytosine = 7400 M^{-1} cm^{-1}.

Chemicals and DNAs

All chemical reagents used were of analytical grade except for dimethyl formamide (DMF) and dioxane, which were spectroscopic grade from

Submitted August 24, 2005, and accepted for publication November 4, 2005.

Address reprint requests to Peter E. Nielsen, Tel.: 45-3-53-27762; Fax: 45-3-53-96042; E-mail: pen@imbg.ku.dk.

0006-3495/06/02/1329/09 $2.00

doi: 10.1529/biophysj.105.073213

Sigma-Aldrich (Munich, Germany). The DNAs were purchased from DNA Technology (Aarhus, Denmark) and used without further purification.

Sample preparation

Main stock solutions of PNAs and DNAs were prepared by dissolution in deionized distilled water. Experimental samples were made by diluting from the corresponding main stock solutions in 10 mM phosphate buffer (pH 7.2) containing 100 mM NaCl and 0.1 mM EDTA for all experiments that required aqueous solvent with medium salt.

Equimolar mixtures (1:1 stoichiometry in single strands) of the PNA or DNA and its complementary strand were dissolved in the buffer mentioned above with the desired concentration of NaCl and the duplexes were prepared by heating these samples up to 90°C and then cooling slowly to the room temperature to allow proper annealing.

UV-melting experiments

The thermal melting experiments were performed on a Cary 300 Bio UV-visible spectrophotometer (Varian, Cary, NC) attached to a temperature controller. Thermal melting profiles were obtained using heating-cooling cycles between 0 and 95°C. The melting temperature (T_m) was determined from the peak of the first derivative of the heating curve. Cuvettes of 1.0 cm pathlength and 1.0 ml volume were used for all these experiments.

Thermodynamics

The thermodynamic parameters, namely, enthalpy change (ΔH^0), entropy change (ΔS^0), and Gibbs' free energy change (ΔG^0), were evaluated using either the hyperchromicity method or the concentration method.

The hyperchromicity method

The hyperchromicity method utilizes α-curve and van 't Hoff plots ($\ln K_T$ versus T^{-1}) according to the following definitions (19): The fraction (α_T) of single strands that remained hybridized in the duplex at a particular temperature T in Kelvin is represented as

$$\alpha_T = \frac{A_s - A}{A_s - A_d}, \tag{1}$$

where A_d is the absorbance of the duplex in fully hybridized condition, A_s is the absorbance of the single strands in fully denatured condition, and A is absorbance at a particular point on the thermal melting curve at temperature T.

For non-self-complementary sequences forming n-mer structures, the general equilibrium equation (K_T) at a particular temperature T can be expressed as

$$K_T = \frac{\alpha_T}{(1-\alpha_T)^n \left(\frac{c_{ts}}{n}\right)^{n-1}}, \tag{2}$$

where c_{ts} represents the total concentration of strands and n is the molecularity of the complex. Assuming a two-state model, Eq. 2 reduces to

$$K_T = \frac{2\alpha_T}{(1-\alpha_T)^2 c_{ts}}. \tag{3}$$

The van 't Hoff plot $\ln K_T$ versus T^{-1} is a straight line represented by

$$\ln K_T = \left(-\frac{\Delta H^0}{R}\right)\frac{1}{T} + \left(\frac{\Delta S^0}{R}\right). \tag{4}$$

Hence, ΔH^0 can be obtained from the slope and ΔS^0 can be obtained from Y-intercept of the van 't Hoff plot. The value ΔG^0 at a particular temperature T in Kelvin can be calculated from

$$\Delta G^0 = -RT\ln K_T = \Delta H^0 - T\Delta S^0, \tag{5}$$

where R is the universal gas constant 1.986 cal/mol.K.

The concentration method

The concentration method utilizes a plot of T_m^{-1} versus lnc_{ts}, where T_m is the thermal melting temperature of the duplex and c_{ts} is the total strand concentration of PNA or DNA.

Since T_m is defined by the temperature where $\alpha = 0.5$ for a two-state transition, combining Eqs. 3 and 4 yields

$$\frac{1}{T_m} = \frac{R}{\Delta H^0}\ln c_{ts} + \frac{\Delta S^0 - R\ln 4}{\Delta H^0}. \tag{6}$$

Thus, the thermodynamic parameters can be extracted from a linear fit to a plot of T_m^{-1} versus lnc_{ts} according to Eq. 6 (19). Hence, ΔH^0 is obtained from the slope of the linear fit and ΔS^0 from the Y-intercept.

The values of the thermodynamics parameter calculated by this method are thus independent of strand concentration, which is not the case with the hyperchromicity method described above.

Evaluation of water activity: calculation of Δn_w

The change in the number of water molecules associated with the thermal melting process of the duplexes, Δn_w, were calculated from the equation (20,21)

$$\Delta n_w = -\frac{\Delta H^0}{nR}\left[\frac{d(T_m^{-1})}{d(\ln a_w)}\right], \tag{7}$$

where n is the number of basepairs in the duplex, R is the universal gas constant, ΔH^0 is the enthalpy change associated with the thermal melting process in pure buffer (aqueous), and a_w is the water activity of the particular solvent. The experimentally determined values of the water activity (lna_w) at given co-solute concentrations were obtained from Rozners and Moulder (21).

Circular dichroism (CD) experiments

CD spectra were scanned in the wavelength range of 200–325 nm, with a response time of 1.0 s, scan speed 200 nm/min, resolution 1.0 nm, and a bandwidth of 1.0 nm on a Jasco J-710 spectropolarimeter (Tokyo, Japan). Each CD spectrum was averaged from 10 accumulations and was corrected for baseline and noise. Cuvettes of 1.0 cm path-length and 1.0 ml volume were used for all of these experiments.

Each sample for CD scan was investigated and characterized by their UV-visible absorption spectrum beforehand. Concentrations of all these samples were in a range as to give an OD of ~1.0 unit at ~260 nm.

RESULTS AND DISCUSSION

It is well established that homopyrimidine PNA oligomers form very stable PNA·DNA·PNA triplexes with complementary DNA oligomers (22). As this would seriously complicate interpretations, we initially chose to study a decameric sequence having only 80% purines (or pyrimidines) in one strand. Thus, PNA and DNA oligomers of the antiparallel sequence pair AGGTAACGAG (seq1)/CTCGTTACCT (seq2) (PNAs 1 and 2 and DNAs 1 and 2 listed in Table 1) have been synthesized for this purpose.

TABLE 1 PNA and DNA sequences

Name	Sequence*†	Base composition
PNA1	H-AGG TAA CGA G-Lys-NH_2	A_4G_4TC
PNA2	H- CTC GTT ACC T-Lys-NH_2	AGT_4C_4
DNA1	5′-AGG TAA CGA G-3′	A_4G_4TC
DNA2	5′-CTC GTT ACC T-3′	AGT_4C_4
PNA3	H-AGT GAA GCA G-Lys-NH_2	A_4G_4TC
PNA4	H-CTG CTT CAC T-Lys-NH_2	AGT_4C_4
DNA3	5′-AGT GAA GCA G-3′	A_4G_4TC
DNA4	5′-CTG CTT CAC T-3′	AGT_4C_4
PNA5	H-GTA GAT CAC T-Lys-NH_2	$A_3G_2T_3C_2$
PNA6	H-AGT GAT CTA C-Lys-NH_2	$A_3G_2T_3C_2$
DNA5	5′-GTA GAT CAC T-3′	$A_3G_2T_3C_2$
DNA6	5′-AGT GAT CTA C-3′	$A_3G_2T_3C_2$

*All the duplexes resulting from these sequences would be antiparallel (either N/C or N/3′ or 5′/3′).

†The N-terminal of the peptide backbone of PNA is shown by an H and the C-terminal (amidated carboxyl terminal) of the peptide backbone of PNA is shown by an NH_2.

The thermal melting and thermodynamic data for all four duplexes PNA1/PNA2, DNA1/DNA2, PNA1/DNA2, and PNA2/DNA1 were determined at a wide range of strand concentrations in aqueous solvent, and the results are presented in Table 2 (representative thermal melting curves are shown in Fig. S1 in the Supplementary Material). Standard enthalpy change (ΔH^0), entropy change (ΔS^0), and free energy change (ΔG^0) values were obtained using the curve fitting, hyperchromicity method (at a duplex concentration of 5.0 μM in strands), and/or the concentration method (T_m^{-1} versus lnc_{ts} plot fitted to Eq. 6; representative plots are shown in Fig. S2 in the Supplementary Material). The two methods showed good agreement. Furthermore, a very good correlation between the relative thermal stability (T_m) and standard free energy change (ΔG^0) as well as to the change in enthalpy (ΔH^0) is observed for the four complexes (Fig. 1). In addition, the system exhibits pronounced enthalpy/entropy compensation behavior. Typically, the PNA·PNA duplex is significantly more stable than the DNA·DNA duplex (~7 kcal/mol), and the PNA·DNA duplexes are both more stable than the DNA·DNA duplex. Most striking, however, is the dramatic difference in stability (~6 kcal/mol) when interchanging the backbones between the two strands in the PNA·DNA duplexes (PNA1·DNA2 versus PNA2·DNA1 duplexes). Clearly, these two duplexes being isosequential have identical basepairing pattern and thus hydrogen-bond contribution to the binding energy. Therefore, the dramatic difference may be sought in differences in counterion binding (and/or release), hydration, and helical structure (resulting in different basepair stacking and backbone conformation) or a combination of these. Additionally, the stabilization could be of kinetic origin if one (or more) of the four oligomers is favorably prestructured in solution before duplex formation. Indeed, it would not be surprising if purines rather than pyrimidines in the PNA strand could favor a helix-poised conformation of the relatively more flexible PNA backbone, and thereby result in faster hybridization kinetics. However, in this case the effect would be expected to be less entropically disfavored, resulting in a relatively higher $\Delta H^0/\Delta S^0$ ratio; but this is clearly not the case.

TABLE 2 Effect of solvent on the duplex properties of PNA1 and PNA2

			T_m^{-1} versus lnc_{ts} plot‡			van 't Hoff plot†			
Strands	Solvent	T_m (°C)*†	ΔG^0_{37} (kcal/mol)	ΔH^0 (kcal/mol)	ΔS^0 (cal/mol.K)	ΔG^0_{37} (kcal/mol)	ΔH^0 (kcal/mol)	ΔS^0 (cal/mol.K)	ΔC_p (kcal/mol.K)¶
	Aqueous‖	65.0 ± 0.2 (5)**	−15.4	−87.6	−233.1	−13.9 ± 0.2 (5)	−74.6 ± 1.8 (5)	−195.8 ± 10.5 (5)	
PNA1·DNA2	50% DMF	44.1 ± 0.3 (3)	−9.3	−63.1	−173.3	−9.5 ± 0.1 (5)	−66.4 ± 1.5 (5)	−183.7 ± 10.6 (5)	1.6
	50% dioxane	51.1 ± 0.2 (3)	−10.8	−64.0	−171.4	−10.7 ± 0.2 (5)	−65.2 ± 2.0 (5)	−175.8 ± 11.0 (5)	
	Aqueous‖	39.0 ± 0.1 (5)††	−8.2	−35.3	−87.4	−8.2 ± 0.1 (5)	−33.7 ± 1.3 (5)	−82.2 ± 4.5 (5)	
PNA2·DNA1	50% DMF	25.1 ± 0.2 (3)	−5.9	−52.6	−150.5	−5.3 ± 0.1 (5)	−59.6 ± 1.5 (5)	−175.0 ± 8.2 (5)	1.3
	50% dioxane	34.1 ± 0.2 (3)	−7.5	−43.9	−117.3	−6.8 ± 0.2 (5)	−52.9 ± 1.5 (5)	−148.5 ± 9.5 (5)	
	Aqueous‖	71.1 ± 0.1 (5)	−16.6	−86.1	−224.0	−15.6 ± 0.2 (5)	−80.5 ± 2.1 (5)	−209.2 ± 11.2 (5)	
PNA1·PNA2	30% DMF	67.3 ± 0.2 (3)	−16.1	−95.8	−256.9	−15.6 ± 0.2 (5)	−87.1 ± 2.0 (5)	−230.5 ± 11.8 (5)	2.5
	50% DMF	65.3 ± 0.1 (3)	−16.7	−105.2	−285.3	−15.4 ± 0.2 (5)	−92.2 ± 2.2 (5)	−247.7 ± 12.0 (5)	
	Aqueous‖	36.2 ± 0.3 (5)	−7.9	−53.4	−146.8	−8.2 ± 0.1 (5)	−53.3 ± 1.5 (5)	−145.4 ± 7.2 (5)	
DNA1·DNA2	30% DMF	20.4 ± 0.1 (3)	−4.5	−62.0	−185.5	−4.3 ± 0.1 (5)	−59.8 ± 2.7 (5)	−179.0 ± 9.3 (5)	1.1
	50% DMF	§	§	§	§	§	§	§	

*The melting temperatures presented are the values obtained at a duplex concentration of 5.0 μM in strands (c_{ts} = 10.0 μM).

†The numbers in parentheses indicate the number of independent measurements used to calculate the standard deviation.

‡Evaluated from a plot of T_m^{-1} versus lnc_{ts} fitted to the Eq. 6 evaluated in a range of 1.0–10.0 μM of strand concentration.

§Could not be measured because of the too low melting temperatures.

¶Specific heat capacity change at constant pressure, $\Delta C_p = \delta\Delta H^0/\delta T_m$, has been calculated in the range of strand concentration 1.0–10.0 μM (Fig. S4), using the theoretical definition published earlier (26).

‖The solvent was 10 mM phosphate buffer containing 100 mM NaCl and 0.1 mM EDTA, pH 7.2 ± 0.01.

**Calculated T_m = 65.1°C (according to Giesen et al. (13)).

††Calculated T_m = 48.8°C (according to Giesen et al. (13)).

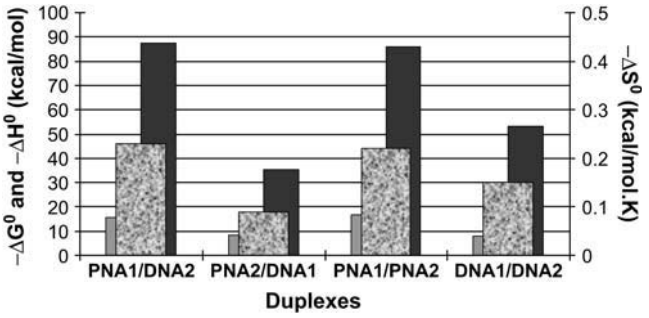

FIGURE 1 A schematic comparison of the values of thermodynamics parameters free energy change (ΔG^0, *shaded*), enthalpy change (ΔH^0, *dark shaded*), and entropy change (ΔS^0, *granite pattern*) for PNA1·PNA2, DNA1·DNA2, PNA1·DNA2, and PNA2·DNA1 duplexes (data from Table 2).

Ionic strength

To address possible differences in counterion binding and/or release, we determined the effect of NaCl concentration on the stabilities of the PNA·DNA duplexes (Fig. 2). These results showed no significant differential effect of the ionic strength. More specifically, the changes in the number of moles of Na^+ ion upon melting of the duplexes are −0.056 for PNA1/DNA2 and −0.053 for PNA2/DNA1 (Table S2 and Fig. S3), which are consistent with the earlier results (23). Therefore, it strongly indicates similar cation binding and release for both the duplexes.

Hydration

Hydration of the pseudopeptide PNA backbone and the phosphodiester DNA backbone are obviously quite different, and within crystal structures of PNA·DNA and PNA·PNA duplexes numerous ordered water molecules have been identified (24,25), many of which specifically contact nucleobases. Therefore specific hydration of the two PNA·DNA duplexes could be quite different and could differently affect the duplex stability.

To address this issue, we studied the effect of organic solvent on duplex stabilities, as this would diminish water activity, and thereby enhance any differential hydration effects. We chose DMF as organic solvent, as this is aprotic but still significantly polar to retain sufficient solubility of the PNA·DNA complexes even at 50% DMF. Interestingly, the results presented in Table 2 show that the presence of DMF has only minor (negative) effect on the PNA·PNA duplex stability (this will be addressed specifically in a subsequent report), whereas the DNA·DNA duplex is significantly destabilized and so are the PNA·DNA duplexes. However, the two PNA·DNA duplexes behave very differently when considering the enthalpic and entropic contributions to the free energy. Although the PNA1·DNA2 duplex is enthalpically destabilized (and thus relatively entropically stabilized), the PNA2·DNA1 duplex is (similarly to but more pronounced than the pure PNA and DNA duplexes) enthalpically stabilized (and thus relatively entropically destabilized); again, resulting in considerable enthalpy/entropy compensation. Fully analogous but somewhat less pronounced results were obtained using dioxane instead of DMF (Table 2).

To corroborate the generality of the above observations, we also analyzed another sequence system with identical base composition but having two basepairs interchanged (seq3/seq4; Table 1). The resulting duplexes of combinations of PNA3, PNA4, DNA3, and DNA4 behaved essentially similar to the seq1/seq2 system in terms of thermal stability and thermodynamics as well as in terms of the effect of DMF (Table 3).

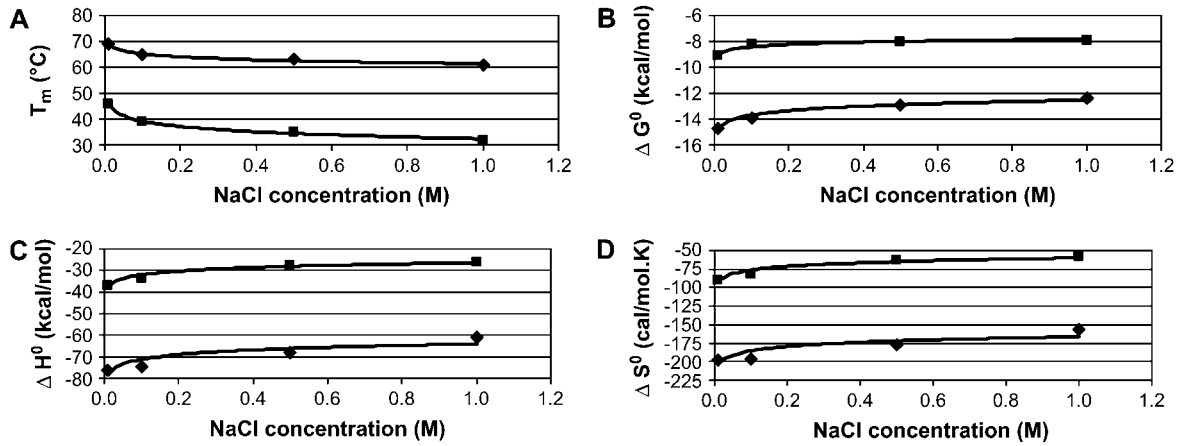

FIGURE 2 Effect of ionic strength (NaCl concentration) on the thermal properties of PNA1·DNA2 (*solid diamond*) and PNA2·DNA1 (*solid square*). The graphs depict the change in T_m (*A*), ΔG^0 (*B*), ΔH^0 (*C*), and ΔS^0 (*D*) as a function of NaCl concentration. The T_m values presented were obtained at a duplex concentration of 5.0 μM in strands (c_{ts} = 10.0 μM). The accuracy of the values of the thermodynamic parameters obtained from the curve fitting in the van't Hoff plot evaluation method was checked by varying the fitting, and the resulted variations in the values were in the range of ±0.1–0.2 kcal/mol for ΔG^0, ±1.0–2.0 kcal/mol for ΔH^0, and ±4.0–12.0 cal/mol.K for ΔS^0.

TABLE 3 Effect of solvent on the duplex properties of PNA3 and PNA4

			T_m^{-1} versus lnc_{ts} plot‡			van 't Hoff plot†			
Strands	Solvent	T_m (°C)*†	ΔG^0_{37} (kcal/mol)	ΔH^0 (kcal/mol)	ΔS^0 (cal/mol.K)	ΔG^0_{37} (kcal/mol)	ΔH^0 (kcal/mol)	ΔS^0 (cal/mol.K)	ΔC_p (kcal/mol.K)§
PNA3·DNA4	Aqueous¶	67.3 ± 0.3 (3)‖	−16.1	−92.4	−245.8	−15.1 ± 0.2 (5)	−86.7 ± 6.8 (5)	−230.8 ± 11.5 (5)	2.5
	50% DMF	46.4 ± 0.2 (3)	−10.4	−83.2	−235.0	−9.8 ± 0.2 (5)	−80.8 ± 5.2 (5)	−228.9 ± 12.3 (5)	
PNA4·DNA3	Aqueous¶	43.3 ± 0.1 (3)**	−8.8	−43.4	−111.7	−8.5 ± 0.1 (5)	−47.9 ± 2.5 (5)	−127.2 ± 7.4 (5)	2.4
	50% DMF	28.4 ± 0.1 (3)	−6.4	−54.0	−153.4	−5.7 ± 0.1 (5)	−73.6 ± 1.5 (5)	−219.1 ± 7.1 (5)	
PNA3·PNA4	Aqueous¶	73.4 ± 0.2 (3)	−17.1	−86.8	−224.7	−15.8 ± 0.2 (5)	−77.5 ± 4.3 (5)	−199.0 ± 6.4 (5)	1.6
	30% DMF	67.4 ± 0.1 (3)	−16.2	−95.6	−246.4	−16.9 ± 0.2 (5)	−101.9 ± 8.4 (5)	−274.3 ± 10.2 (5)	
DNA3·DNA4	Aqueous¶	40.6 ± 0.09 (3)	−8.6	−56.7	−155.1	−8.4 ± 0.1 (5)	−55.4 ± 3.2 (5)	−151.6 ± 9.2 (5)	2.4
	30% DMF	23.3 ± 0.1 (3)	−5.0	−64.0	−190.2	−5.1 ± 0.1 (5)	−62.9 ± 5.5 (5)	−186.5 ± 6.5 (5)	

*The melting temperatures presented are the values obtained at a duplex concentration of 5.0 μM in strands (c_{ts} = 10.0 μM).
†The numbers in parentheses indicate the number of independent measurements used to calculate the standard deviation.
‡Evaluated from a plot of T_m^{-1} versus lnc_{ts} fitted to the Eq. 6 evaluated in a range of 1.0–10.0 μM of strand concentration.
§Specific heat capacity change at constant pressure, $\Delta C_p = \delta\Delta H^0/\delta T_m$, has been calculated in the range of strand concentration 1.0–10.0 μM (Fig. S5), using the theoretical definition published earlier (26).
¶The solvent was 10 mM phosphate buffer containing 100 mM NaCl and 0.1 mM EDTA, pH 7.2 ± 0.01.
‖Calculated T_m = 65.6°C (according to Giesen et al. (13)).
**Calculated T_m = 49.3°C (according to Giesen et al. (13)).

Finally, we studied a fully purine/pyrimidine mixed sequence (seq5/seq6; Table 1) as a control. As expected, the PNA·PNA duplex in this system is significantly more stable than the other duplexes, but both of the PNA·DNA duplexes (PNA5·DNA6 and PNA6·DNA5) exhibit virtually identical thermal stability as well as thermodynamic parameters, and both are significantly more stable than the DNA·DNA duplex (Table 4).

The influence of organic solvent on the thermodynamic properties of these purine/pyrimidine strand asymmetric PNA·DNA duplexes is quite remarkable (Tables 2 and 3). Whereas the difference in free energy ($\Delta\Delta G^0$) quite closely follows the difference in thermal stability between the homologous duplexes containing purine-rich and pyrimidine-rich PNA strands in pure aqueous medium as well as in 50% organic solvent, this is not the case for either the enthalpy or the entropy differences (Tables 2 and 3). In fact, the differences in enthalpies and entropies of duplex formation between the two backbone-interchanged duplexes are much smaller in organic solvent as compared to pure aqueous medium.

Specific heat capacity change (enthalpic)

Changes in specific heat capacity could affect our conclusions. Therefore, we evaluated the specific heat capacity change at constant pressure (ΔC_p) for all the complexes of seq1/seq2, seq3/seq4, and seq5/seq6, from the concentration dependence of thermal melting temperature and enthalpy change using published procedures (26). The values are in

TABLE 4 Effect of solvent on the duplex properties of PNA5 and PNA6

			T_m^{-1} versus lnc_{ts} plot‡			van 't Hoff plot†			
Strands	Solvent	T_m (°C)*†	ΔG^0_{37} (kcal/mol)	ΔH^0 (kcal/mol)	ΔS^0 (cal/mol.K)	ΔG^0_{37} (kcal/mol)	ΔH^0 (kcal/mol)	ΔS^0 (cal/mol.K)	ΔC_p (kcal/mol.K)§
PNA5·DNA6	Aqueous¶	51.3 ± 0.09 (3)‖	−11.3	−73.0	−199.2	−10.6 ± 0.2 (5)	−68.1 ± 4.2 (5)	−185.4 ± 10.3 (5)	1.4
	50% DMF	31.1 ± 0.1 (3)	−6.8	−61.0	−174.7	−6.5 ± 0.1 (5)	−59.6 ± 2.7 (5)	−171.0 ± 11.4 (5)	
PNA6·DNA5	Aqueous¶	50.4 ± 0.08 (3)**	−11.0	−72.6	−198.6	−10.6 ± 0.2 (5)	−71.6 ± 1.6 (5)	−196.6 ± 12.2 (5)	1.9
	50% DMF	29.6 ± 0.2 (3)	−6.3	−64.4	−187.2	−6.4 ± 0.1 (5)	−65.3 ± 1.4 (5)	−190.1 ± 9.7 (5)	
PNA5·PNA6	Aqueous¶	70.3 ± 0.1 (3)	−17.2	−96.6	−256.2	−17.6 ± 0.2 (5)	−102.4 ± 1.5 (5)	−273.4 ± 9.5 (5)	2.0
	30% DMF	64.3 ± 0.1 (3)	−15.6	−94.3	−253.7	−14.5 ± 0.2 (5)	−85.4 ± 2.4 (5)	−228.7 ± 9.5 (5)	
DNA5·DNA6	Aqueous¶	36.3 ± 0.3 (3)	−7.7	−69.0	−197.6	−8.2 ± 0.1 (5)	−71.0 ± 3.3 (5)	−202.4 ± 8.8 (5)	1.8
	30% DMF	18.3 ± 0.2 (3)	−3.9	−63.9	−193.5	−3.7 ± 0.1 (5)	−64.2 ± 3.1 (5)	−195.0 ± 8.9 (5)	

*The melting temperatures presented are the values obtained at a duplex concentration of 5.0 μM in strands (c_{ts} = 10.0 μM).
†The numbers in parentheses indicate the number of independent measurements used to calculate the standard deviation.
‡Evaluated from a plot of T_m^{-1} versus lnc_{ts} fitted to the Eq. 6 evaluated in a range of 1.0–10.0 μM of strand concentration.
§Specific heat capacity change at constant pressure, $\Delta C_p = \delta\Delta H^0/\delta T_m$, has been calculated in the range of strand concentration 1.0–10.0 μM (Fig. S6), using the theoretical definition published earlier (26).
¶The solvent was 10 mM phosphate buffer containing 100 mM NaCl and 0.1 mM EDTA, pH 7.2 ± 0.01.
‖Calculated T_m = 50.8°C (according to Giesen et al. (13)).
**Calculated T_m = 50.8°C (according to Giesen et al. (13)).

the range of 1.0–2.5 (Tables 2–4, Figs. S4–S6), and no systematic differences in ΔC_p are apparent between the duplexes. In particular, the differences between the two control duplexes, PNA5·DNA6/PNA6·DNA5, are as large as those between the asymmetric duplexes PNA1 · DNA2/PNA2 · DNA1, indicating that differences in ΔC_p cannot be the reason of the differential stabilities of these duplexes.

Water activity

The obvious differential effect of aqueous versus organic solvent on the behavior of the PNA1·DNA2 and PNA2·DNA1 duplexes immediately suggests that these duplexes are differently hydrated, and that the difference in hydration is influencing or could even be responsible for their vastly different stability. To explore further the contribution of the extent of hydration of the purine-rich PNA compared to the purine-rich DNA, the change in number of bound water molecules in the thermal melting process was determined using a method described by others (20,21) employing manipulation of the water activity by addition of the low molecular weight co-solutes ethylene glycol and glycerol.

Fig. 3 shows that both ethylene glycol and glycerol cause considerable depression in the thermal melting temperature of the DNA1·DNA2 duplex. The values of Δn_w (Eq. 7) are 3.5 and 6.4 in ethylene glycol and glycerol, respectively (Table 5), which is close to the values obtained by Spink and Chaires (20) and Rozner and Moulder (21). On the other hand, the other three duplexes that involve PNA strands PNA1·PNA2, PNA1·DNA2, and PNA2·DNA1 showed very little change in their melting temperature with increasing concentration of ethylene glycol or glycerol (Fig. 3). The values of Δn_w obtained in these cases are in the range of 0 to 1.0, which implies that there is little change in the number of bound water molecules during the thermal melting process of these duplexes (Table 5). Thus, differences in bound water can hardly explain the differential behavior of the PNA·DNA duplexes.

CD spectroscopy analysis

To investigate whether structural differences between or conformational changes within the duplexes could explain their behavior, we resorted to CD spectroscopy. Fig. 4 represents a comparison between the CD spectra of all four duplexes of seq1/seq2 (Fig. 4 *A*) and all four duplexes of seq3/seq4 (Fig. 4 *B*) in aqueous solvent. These data based on spectral similarities and differences would indicate that while the two DNA duplexes DNA1·DNA2 and DNA3·DNA4 have quite similar helical structures, the helical structures of the four PNA duplexes differ much more from that of the DNA as well as from each other. This is in accordance with previous structural data obtained by NMR, x-ray crystallography, and CD spectroscopy (5,12,25,27,28). In particular, the CD spectrum of the PNA2·DNA1 duplex (containing pyrimidine-rich PNA), which is characterized by three close maxima in the range of 250–275 nm, appears distinct, whereas that of the PNA1·DNA2 duplex (containing purine-rich PNA) is much closer to that of the corresponding DNA1·DNA2 (Fig. 4 *A*). In contrast, however, the CD spectrum of the PNA4·DNA3 duplex (containing pyrimidine-rich PNA) resembles that of the corresponding DNA duplex more than that of the PNA3·DNA4 duplex (Fig. 4 *B*). Therefore, these results do not support the existence of a unique structure related to either purine-rich or pyrimidine-rich PNA in the PNA·DNA duplexes.

We also investigated circular dichroic properties of PNA·DNA duplexes (seq1/seq2) in organic solvent (dioxane

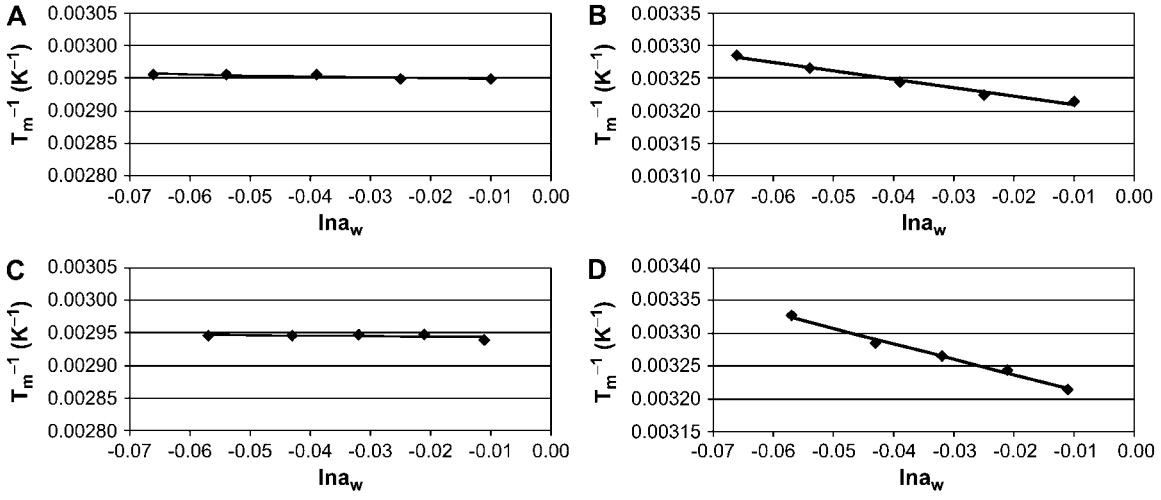

FIGURE 3 Plots of reciprocal thermal melting temperatures of DNA1·DNA2 (*B* and *D*) and PNA1·DNA2 (*A* and *C*) as a function of the logarithm of water activity (lna_w) at different co-solute concentrations for ethylene glycol (*A* and *B*) and glycerol (*C* and *D*). T_m values were measured at a duplex concentration 5.0 μM in strands at 0%, 5%, 10%, 15%, or 20% ethylene glycol or glycerol in 10 mM phosphate buffer containing 100 mM NaCl and 0.1 mM EDTA, pH 7.2 $\pm$ 0.01. The experimentally determined values of lna_w at given co-solute concentrations have been taken from Rozners and Moulder (21).

TABLE 5 Estimation of the change in the number of bound water molecules associated with the thermal melting of the duplexes

Duplex	Δn_w*†‡	
	Ethylene glycol§	Glycerol§
PNA1·DNA2	0.64	0.37
PNA2·DNA1	−0.74	−0.44
PNA1·PNA2	0.59	0.45
DNA1·DNA2	3.48	6.37

*Values of Δn_w have been calculated using the values of the slopes of the plots in Fig. 3 fitted to Eq. 7.
†ΔH^0 value varies only slightly with the nature and concentration of the small co-solutes (C.H. Spink and J.B. Chaires, personal communication) and enthalpy-entropy compensation takes place. Therefore, it was assumed that such variation in ΔH^0 values can be excluded from the calculation using Eq. 7 and ΔH^0 value in pure buffer (aqueous) will be used instead.
‡These Δn_w values are not absolute values.
§The range of co-solute concentration in the experiments was 5–20%.

rather than DMF, due to absorbance interference of the latter) to address whether the effects of aprotic organic solvent include structural changes of the helix. Fig. 5 represents a comparison between the CD spectra of PNA1·DNA2 and PNA2·DNA1 in aqueous solvent as well as in 50% dioxane.

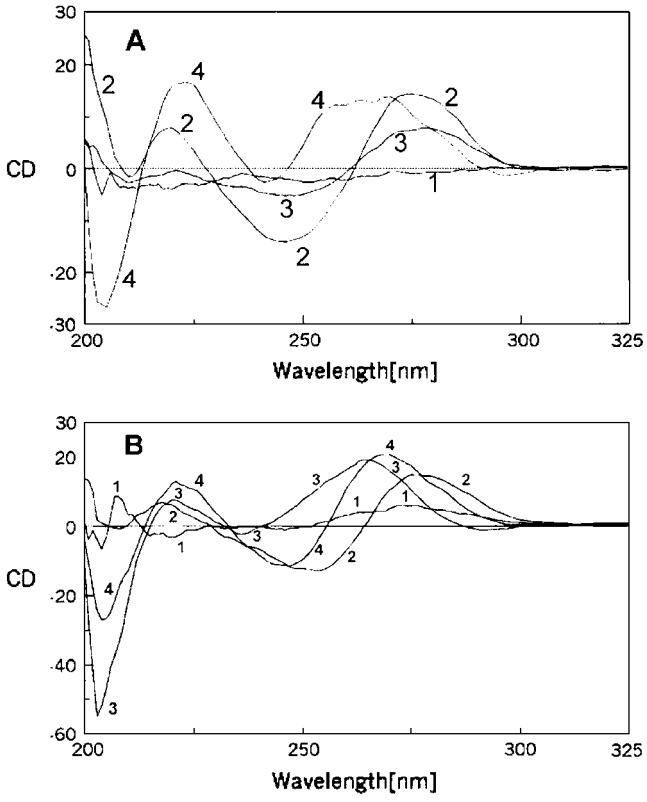

FIGURE 4 CD spectra in aqueous solvent. (*A*) CD spectra of PNA1·PNA2 (*curve 1*), DNA1·DNA2 (*curve 2*), PNA1·DNA2 (*curve 3*), and PNA2·DNA1 (*curve 4*). (*B*) CD spectra of PNA3·PNA4 (*curve 1*), DNA3·DNA4 (*curve 2*), PNA3·DNA4 (*curve 3*), and PNA4·DNA3 (*curve 4*). All the duplexes were 6.0 μM in strands. The solvent was 10 mM phosphate buffer containing 100 mM NaCl and 0.1 mM EDTA, pH 7.2 ± 0.01 at 22°C.

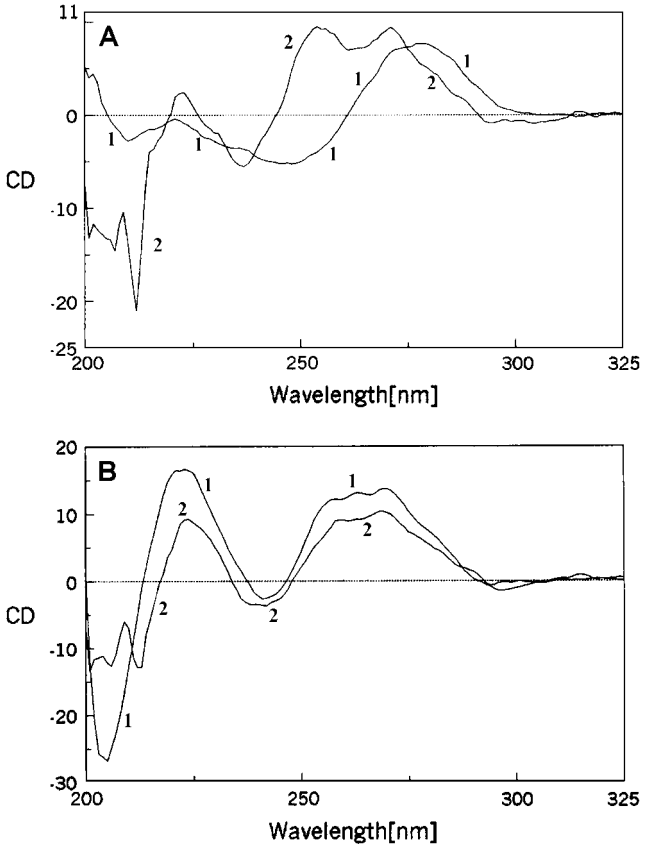

FIGURE 5 Comparison of CD spectra in nonaqueous solvent with those in aqueous solvent at 22°C. (*A*) CD spectra of PNA1·DNA2 in aqueous solvent (*curve 1*) and in 50% dioxane (*curve 2*). (*B*) CD spectra of PNA2·DNA1 in aqueous solvent (*curve 1*) and in 50% dioxane (*curve 2*). The duplexes were 6.0 μM in strands. The aqueous solvent was 10 mM sodium phosphate buffer containing 100 mM NaCl and 0.1 mM EDTA, pH 7.2 ± 0.01.

Interestingly, very little change is observed for the PNA2·DNA1 duplex (Fig. 5 *B*), whereas the CD spectrum of the PNA1·DNA2 duplex was significantly changed in 50% dioxane (Fig. 5 *A*). In fact, the spectrum of PNA1·DNA2 under this condition (50% dioxane) is quite similar to that of the PNA2·DNA1 duplex both in pure aqueous solvent and 50% dioxane. Therefore the CD results could indicate that the PNA1·DNA2 duplex that contains purine-rich PNA adopts a distinct structure in aqueous solution, but reverts to a more common duplex structure at lower water activity (partly organic solvent). This, however, cannot be a general feature of the duplexes containing purine-rich PNA, since a similar conformational difference is not indicated by the CD spectra of the PNA3·DNA4 and PNA4·DNA3 duplexes in pure aqueous solvent (Fig. 4 *B*), considering the contention that circular dichroic spectra predominantly reflect the helical structure of the duplex along with the stacking of the nucleobases.

Nonetheless, the CD results would indicate a structural basis for the differential behavior of the PNA·DNA duplexes, the origin of which might be sought in the structural

differences of the backbone linked to the purine/pyrimidine nucleobases. For this purpose, we compared the dihedral angles of A, T, G, and C nucleobases for the three typical bonds N1′-N4′, C3′-C′, and C8′-C5′ in the available structure of a self-complementary PNA hexamer (25) (Table S1 in the Supplementary Material). However, this analysis did not reveal any significant systematic differences between purine and pyrimidine bases linked to the PNA backbone.

CONCLUSIONS

These results strongly corroborate and expand earlier conclusions (14,15) that the stability of PNA·DNA duplexes exhibits a very pronounced dependence on the relative purine content of the PNA strand. The effect is dramatic considering that the chemical exercise essentially consists of the switching of the two backbones on the same stack of nucleobasepairs. Clearly, this should not affect basepairing, but could affect helical structure through backbone-nucleobase interactions (including basepair stacking), counterion binding, solvation, single-strand stability, and structure.

Based on our data, we find it unlikely that differences in counterion binding (identical ionic-strength dependence was observed), hydration (identical and insignificant water release was observed), or single-strand conformation can be responsible for the difference in duplex stability. The CD spectroscopy data do indicate differences in the structure (stacking) between the helices, but this does not appear to be a consistent feature with regard to sequence changes (comparing seq1/seq2 and seq3/seq4 systems).

The only consistent difference observed between the purine-rich PNA versus the pyrimidine-rich PNA in isosequential PNA·DNA duplexes is the significant increase in both binding enthalpy and entropy (and thus the relative enthalpic contribution to the free energy) for the PNA·DNA duplexes containing pyrimidine-rich PNA (PNA2·DNA1 and PNA4·DNA3) in organic solvent, which would indicate that these duplexes are relatively enthalpically disfavored in water.

Although our results so far do not allow us to identify the origin of the different stabilities of homopurine/homopyrimidine PNA·DNA duplexes, the evidence does point to a significant structural component, which involves enthalpic contributions both within the duplex structure as well as from bound water molecules.

Overall, it can be concluded that seemingly subtle and not easily measurable and explainable differences in helical/structural properties may have profound influence on thermodynamic stability and behavior. These results should inspire more exact structural (NMR or crystallographic) as well as molecular modeling and simulation studies on these systems to seek a structurally based explanation.

SUPPLEMENTARY MATERIAL

An online supplement to this article can be found by visiting BJ Online at http://www.biophysj.org.

We express our sincere gratitude to Prof. S. Harnung, Dept. of Chemistry, University of Copenhagen, for access to the CD spectrophotometer.

This work was supported by the European Commission (Sixth Framework PACE project).

REFERENCES

1. Nielsen, P. E. 2001. Peptide nucleic acid targeting of double-stranded DNA. *Methods Enzymol.* 340:329–340.
2. Nielsen, P. E. 2001. Targeting double-stranded DNA with peptide nucleic acid (PNA). *Curr. Med. Chem.* 8:545–550.
3. Nielsen, P. E. 2001. Peptide nucleic acid: a versatile tool in genetic diagnostics and molecular biology. *Curr. Opin. Biotechnol.* 12: 16–20.
4. Ray, A., and B. Nordén. 2000. Peptide nucleic acid (PNA): its medical and biotechnical applications and promise for the future. *FASEB J.* 14:1041–1060.
5. Egholm, M., O. Buchardt, L. Christensen, C. Behrens, S. M. Freier, D. A. Driver, R. H. Berg, S. K. Kim, B. Nordén, and P. E. Nielsen. 1993. PNA hybridizes to complementary oligonucleotides obeying the Watson-Crick hydrogen-bonding rules. *Nature.* 365:566–568.
6. Griffin, T. J., and L. M. Smith. 1998. An approach to predicting the stabilities of peptide nucleic acid·DNA duplexes. *Anal. Biochem.* 260: 56–63.
7. Ratilainen, T., A. Holmén, E. Tuite, G. Haaima, L. Christensen, P. E. Nielsen, and B. Nordén. 1998. Hybridization of peptide nucleic acid. *Biochemistry.* 37:12331–12342.
8. Chakrabarti, M. C., and F. P. Schwarz. 1999. Thermal stability of PNA/DNA and DNA/DNA duplexes by differential scanning calorimetry. *Nucleic Acids Res.* 27:4801–4806.
9. Schwarz, F. P., S. Robinson, and J. M. Butler. 1999. Thermodynamic comparison of PNA/DNA and DNA/DNA hybridization reactions at ambient temperature. *Nucleic Acids Res.* 27:4792–4800.
10. Ratilainen, T., A. Holmén, E. Tuite, P. E. Nielsen, and B. Nordén. 2000. Thermodynamics of sequence-specific binding of PNA to DNA. *Biochemistry.* 39:7781–7791.
11. Sugimoto, N., N. Satoh, K. Yasuda, and S. Nakano. 2001. Stabilization factors affecting duplex formation of peptide nucleic acid with DNA. *Biochemistry.* 40:8444–8451.
12. Tomac, S., M. Sarkar, T. Ratilainen, P. Wittung, P. E. Nielsen, B. Nordén, and A. Gräslund. 1996. Ionic effects on the stability and conformation of peptide nucleic acid complexes. *J. Am. Chem. Soc.* 118:5544–5552.
13. Giesen, U., W. Kleider, C. Berding, A. Geiger, H. Orum, and P. E. Nielsen. 1998. A formula for thermal stability (T_m) prediction of PNA/DNA duplexes. *Nucleic Acids Res.* 26:5004–5006.
14. Nielsen, P. E., and L. Christensen. 1996. Strand displacement binding of a duplex-forming homopurine PNA to a homopyrimidine duplex DNA target. *J. Am. Chem. Soc.* 118:2287–2288.
15. Christensen, L., H. F. Hansen, T. Koch, and P. E. Nielsen. 1998. Inhibition of PNA triplex formation by N4-benzoylated cytosine. *Nucleic Acids Res.* 26:2735–2739.
16. Gyi, J. I., G. L. Conn, A. N. Lane, and T. Brown. 1996. Comparison of the thermodynamic stabilities and solution conformations of DNA·RNA hybrids containing purine-rich and pyrimidine-rich strands with DNA and RNA duplexes. *Biochemistry.* 35:12538–12548.
17. Gyi, J. I., A. N. Lane, G. L. Conn, and T. Brown. 1998. Solution structures of DNA.RNA hybrids with purine-rich and pyrimidine-rich strands: comparison with the homologous DNA and RNA duplexes. *Biochemistry.* 37:73–80.
18. Christensen, L., R. Fitzpatrick, B. Gildea, K. Petersen, H. F. Hansen, T. Koch, M. Egholm, O. Buchardt, P. E. Nielsen, J. Coull, and R. Berg. 1995. Solid-phase synthesis of peptide nucleic acids. *J. Pept. Sci.* 1: 175–183.

19. Peyret, N., P. A. Seneviratne, H. T. Allawi, and J. SantaLucia, Jr. 1999. Nearest-neighbor thermodynamics and NMR of DNA sequences with internal A·A, C·C, G·G, and T·T mismatches. *Biochemistry.* 38:3468–3477.

20. Spink, C. H., and J. B. Chaires. 1999. Effects of hydration, ion release, and excluded volume on the melting of triplex and duplex DNA. *Biochemistry.* 38:496–508.

21. Rozners, E., and J. Moulder. 2004. Hydration of short DNA, RNA and 2′-OMe oligonucleotides determined by osmotic stressing. *Nucleic Acids Res.* 32:248–254.

22. Krupnik, O. V., Y. A. Guscho, K. A. Sluchanko, P. E. Nielsen, and Y. S. Lazurkin. 2001. Thermodynamics of the melting of PNA_2/DNA triple helices. *J. Biomol. Struct. Dyn.* 19:535–542.

23. Tomac, S., M. Sarkar, T. Ratilainen, P. Wittung, P. E. Nielsen, B. Nordén, and A. Gräslund. 1996. Ionic effects on the stability and conformation of peptide nucleic acid complexes. *J. Am. Chem. Soc.* 118:5544–5552.

24. Menchise, V., G. De Simone, T. Tedeschi, R. Corradini, S. Sforza, R. Marchelli, D. Capasso, M. Saviano, and C. Pedone. 2003. Insights into peptide nucleic acid (PNA) structural features: the crystal structure of a D-lysine-based chiral PNA-DNA duplex. *Proc. Natl. Acad. Sci. USA.* 100:12021–12026.

25. Rasmussen, H., J. S. Kastrup, J. M. Nielsen, and P. E. Nielsen. 1997. Crystal structure of a peptide nucleic acid (PNA) duplex at 1.7 Å resolution. *Nat. Struct. Biol.* 4:98–101.

26. Wu, P., S. Nakano, and N. Sugimoto. 2002. Temperature dependence of thermodynamics properties for DNA/DNA and RNA/DNA duplex formation. *Eur. J. Biochem.* 269:2821–2830.

27. Leijon, M., A. Gräslund, P. E. Nielsen, O. Buchardt, B. Nordén, S. M. Kristensen, and M. Eriksson. 1994. Structural characterization of PNA-DNA duplexes by NMR. Evidence for DNA in a B-like conformation. *Biochemistry.* 33:9820–9825.

28. Eriksson, M., and P. E. Nielsen. 1996. Solution structure of a peptide nucleic acid-DNA duplex. *Nat. Struct. Biol.* 3:410–413.